11th World Congress on Computational Mechanics (WCCM XI)
5th European Conference on Computational Mechanics (ECCM V)
6th European Conference on Computational Fluid Dynamics (ECFD VI)
E. Oñate, J. Oliver and A. Huerta (Eds)

THE INFLUENCE OF MUSCLE MODELING METHODS AND PATHS ON HEAD AND NECK RESPONSE

COURTNEY A. COX*, ALAN T. DIBB*, HATTIE C. CUTCLIFFE*, ROGER W. NIGHTINGALE*, BARRY S. MYERS*, ANITA N. VASAVADA†, BETHANY L. SUDERMAN†, AND CAMERON R. 'DALE' BASS*

* Department of Biomedical Engineering
Duke University
136 Hudson Hall Box 90281, Durham NC, 27708
e-mail: courtney.a.cox@duke.edu

† Washington State University
118 Dana Hall Spokane St., P.O. Box 642710
Pullman, WA 99164

Key Words: *Biomechanics, Cervical Spine, Muscle Wrapping, Computational Models*

Abstract. *For inertial loading in frontal impacts, the effects of the neck muscles are profound, and impact the accuracy of computational and physical surrogates. Previous studies have shown two important aspects of muscle modeling in adult computational models are muscle attachment location and muscle loading lines of action. The objective of the current study was to evaluate techniques for modeling muscle curvature in adult computational neck muscles using data from cadaveric dissections and MRI, and to investigate the changes in overall head/neck response when using different muscle wrapping techniques. Dissection based muscle paths were modeled using multiple linear muscle strands, which resulted in curved loading lines of action similar to the MRI derived muscle paths. Six of the 12 muscles had a portion of their paths, (on average 25±14% of the path length), that were significantly different from the MRI derived paths. Muscles that incorporated muscle wrapping with sliding contact interactions resulted in the highest correlation to volunteer kinematic corridors in a 15 G frontal impact. This curvilinear muscle response should be included to improve model response for frontal impact with muscle activation.*

1 INTRODUCTION

For inertial loading in frontal impacts, the effects of the neck muscles are profound. Computational models using finite element (FE) and multibody dynamics have shown that the most important modeling parameters dictating head kinematics are the muscle's constitutive properties, locations, line-of-action, activation level, and activation timing [1-5]. A tensed muscle response may contribute 40% or more of the compressive tolerance of the adult and pediatric neck [6]. A sensitivity analysis by Dibb, 2011 found muscle attachment locations

were among the top four variables affecting head kinematics. Improving the accuracy of muscle geometries and kinematics constitutive properties represents an opportunity to enhance overall model performance.

A major challenge in computational neck models is the limited quantitative data on muscle geometry. A cadaveric cervical dissection study [7,8] reported detailed insertion, origin, volume, and length data from six 50^{th} percentile adult male subjects that has been used in several neck models. As no curvature was reported of the dissected muscles, models relying on this dissection data generally employ muscles that act directly from insertion to origin, not along the curved muscle paths seen in human necks. Another source of muscle geometry is MRI-based, and reports curved muscle paths based on the centroids of cross-sectional areas at different levels throughout the volume of a muscle [9-11]. However muscle insertions and origins are difficult to accurately determine from MRI. To date, no study has been conducted to evaluate muscle modeling techniques using origin, insertion, and centroidal path data derived from both cadaveric dissections and magnetic resonance imaging (MRI).

A second challenge for head and neck models is modeling interactions between the musculature and osteoligamentous spine. Cervical muscles wrap around each other and vertebrae during head extension and flexion. Some models avoided this problem by either excluding neck muscles or lumping muscle stiffness into the osteoligamentous joints. This approach has limitations since it ignores the effect of the loading line of action of the muscle on the vertebrae and head. More recently, models have included muscles as single-segment one-dimensional elements, which are only able to interact with the spine at their connected endpoints. If the head is loaded in a manner that results in large neck bending, the muscle line-of-action may pass through the underlying osteoligamentous spine resulting in non-physiological forces in the neck.

Methods to solve this muscle interaction problem can be classified in one of three categories: solid or shell element muscles, multi-segmented one-dimensional muscle elements, or sliding contact interaction one-dimensional elements. Using shell or solid elements is computationally expensive and, to date, lacks the ability to model active contractile muscle properties [12-14]. The multi-segment method divides the muscle into discrete segments of one-dimensional elements. The intersegmental nodes are then rigidly attached to adjacent vertebra which maintains a fixed distance between the osteoligamentous spine and the muscular spine. The sliding contact interaction allows for a continuous model that interacts with the vertebrae at specific locations through guide nodes [3,15-22]. In order to maintain an anatomically correct relationship between the muscle and the cervical spine, these nodes need not be in physical contact with the vertebrae. A contact interaction called *CONTACT_GUIDED_CABLE released by LSTC (Livermore, CA) can be used as a sliding contact to model muscular wrapping in LS-DYNA. This contact interaction allows for sliding friction and contact stiffness to be defined. In addition, it uses beam elements, which can be assigned the appropriate muscular section properties, constitutive properties, and activations.

This study's objective was to evaluate techniques for modeling muscle curvature in the adult neck using data from cadaver dissections and MRI, and to investigate the changes in overall head/neck response when using different muscle wrapping techniques. It was hypothesized that muscle models incorporating both multi-segments, as well as the potential for sliding contact interactions, would produce results that are more correlated to volunteer responses in terms of muscle pathways and kinematic responses.

2 METHODS

2.1 Model development

The model used in this study (Figure 1) is a hybrid multibody and finite element computational model of the adult 50th percentile male. It consists of an osteoligamentous cervical spine (C1/C2, C3 to T1) and head, modeled as rigid bodies coupled by six degree of freedom non-linear viscoelastic beam intervertebral joints (Occiput-C2, C2-C3, to C7-T1). The model includes 22 primary cervical spine muscles, which are split into 81 muscle strands to span their broad origins and insertions. Each muscle strand was modeled with two parallel rate sensitive beam elements to capture the active and passive muscle behaviors. Further muscle modeling details can be found in Dibb 2011. The design and development of this version of the model is detailed by Dibb (2011, 2014, 2013). Model simulations were performed using LS-DYNA, version 971 R6 (LSTC, Livermore, CA).

2.2 Muscle wrapping techniques

To investigate the effect of wrapping, three muscle models (Figure 1) were implemented to simulate the interactions of muscle, vertebra, and other soft tissue during bending. The first used single-segment muscles with limited interactions between the muscle and the osteoligamentous spine, at only the muscle origin and insertion locations. The origin and insertion locations were measured from the dissection of six cadavers [8]. The second muscle model used multi-segment muscles, in which each muscle was divided serially into segments. For every vertebra spanned, the muscle strand was segmented and the intersegmental node was rigidly attached to the spanned vertebra. The intersegmental nodes of a muscle lay on the (straight) insertion to origin vector and were vertically located at the same height as the vertebral center of gravity. The third model used a sliding contact interaction between the muscles and the vertebrae. Each muscle strand was divided serially into 12 segments of equal length. A series of guiding nodes, implemented using the same method as in the multi-segment model in conjunction with LSTC's contact guided cable interaction, allowed for the muscle to slide past the node. The default frictionless contact interaction was used between the muscle element and the guide node.

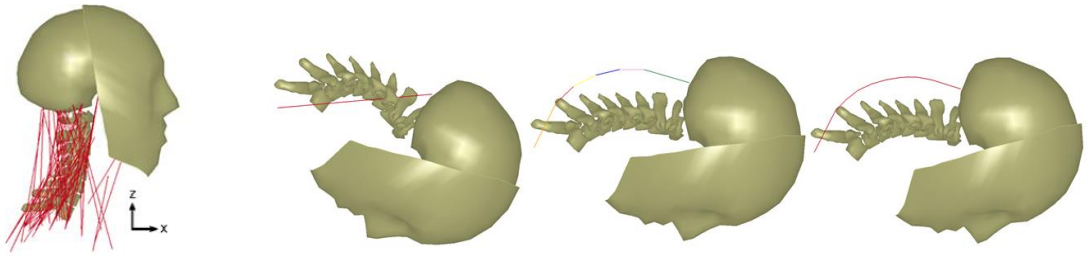

Figure 1: a. Lateral view of the adult head and neck model, which includes 22 muscles. b. Single-segment (left), multi-segment (center), and sliding contact (right) muscle strand during a flexed position. The nodes defining the muscle paths of the sliding contact and multi-segment models were rigidly attached to the adjacent vertebrae.

Muscle paths

As the positions of the muscles relative to the vertebrae and each other change as the head rotates from extension to flexion, an important step was to validate the modeled muscle paths with anatomically correct paths. To do so, the MRI derived spinal muscle paths from Vasavada et al. [9] were compared with the paths from our model. Vasavada et al. computed the paths of 12 muscles from a single volunteer in flexed, neutral, and extended postures. The muscles were identified and outlined in sequential axial MR images and the consecutive centroids of each cross-sectional area for each muscle were connected to define a piece-wise linear muscle path.

Since the muscles in the model of the current study are made up of multiple strands, derivation of a centroidal path for the modeled muscles was necessary to make comparisons. This was possible because the muscle strand data in the model was calculated from previously published cadaver data [7,8]. For each cadaver, an aggregate muscle path from the multiple strands of each muscle was created through weighted averaging based on physiological cross sectional area (PCSA) of each strand (Figure 2). The x and y coordinates of each strand were averaged together relative to their PCSA along the entire length of the muscle. A statistical corridor for each path was created based on the standard deviations of the reported origin and insertion points from the dissections.

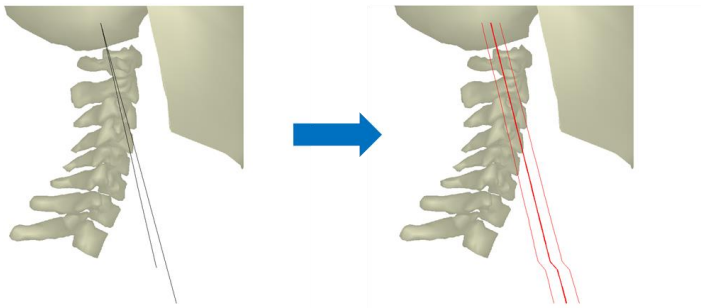

Figure 2: An aggregate muscle path corridor (right) was created through a weighted average of muscle strand pathways based on PCSA (left). The corridor is developed from the standard deviations in the origin and insertion points in the cadaver data.

To evaluate the muscle paths, simulations were run duplicating the kinematics of Vasavada et al (2008). This was accomplished by prescribing rigid body rotation to the head and vertebrae to achieve 30° flexed, neutral, and 30° extended head and neck postures with kinematics independent of the muscle models. Comparisons between model and MRI data were made using an error metric based on the average transverse plane length between the paths. Two-sided Student's t-tests were used to test for significant differences ($p < 0.05$) in error metric between paths. The effect of muscle wrapping on muscle line of action was studied by comparing paths from the three different muscle models during head and neck flexion and extension. Muscle model statistical significance was tested through two factor ANOVA (where factors were muscle model and flexion/extension) with a significance level of $p=0.05$.

15 G frontal impact

An adult volunteer 15 G frontal impact [23,24] was simulated in order to verify model biofidelity, and to compare the three muscle wrapping techniques. Average T1 x-direction accelerations and y-direction rotational displacements from the volunteer tests [23] were applied to the T1 vertebrae of the models. Model response was compared to volunteer corridors through a correlation analysis, which was a linear combination of a corridor method and a cross-correlation method [6,24-26]. Correlation scores quantified how well the model response fit within the volunteer corridor, and how well the magnitude, phase shift, and shape of the model response matched the volunteer corridor. The global correlation score was the mean of the correlation scores for peak head rotational displacement, neck rotational displacement, head rotational acceleration, head x-directional displacement, head z-directional displacement, and head linear acceleration. Further details of model simulations with the 15 G frontal impact can be found in Dibb et al. 2014.

In this study, two different muscle activation schemes were investigated as follows:

1. Relaxed activation state: represents an unaware subject [6,27]. Activations for each muscle were less than ten percent and were optimized for the sliding contact muscles.
2. Full extensor activation state: represents the maximum possible resistance to flexion. Muscles were initiated with a relaxed activation state and all extensor muscles were activated to 100 percent upon impact [5].

Each activation scheme was assigned to the three muscle wrapping techniques. The peak kinematic model responses were output for each simulation, along with the Head Injury Criterion (HIC) value.

3 RESULTS

3.1 Muscle paths

Muscle paths derived from cadaveric dissections and modeled using multiple linear muscle strands resulted in curved loading lines of action similar to the MRI derived muscle paths from Vasavada et al. (2008). Paths for the sternocleidomastoid and splenius cervicis are presented in Figure 3. Six of the 12 muscles had a portion of their paths (on average 25±14% of the path length), that were significantly different ($p<0.05$) from the MRI derived paths (i.e., the corridor did not include the MRI path). The specific muscles exhibiting these differences were the longissimus cervicis, scalenus anterior, semispinalis cervicis, splenius cervicis, sternocleidomastoid, and trapezius. The average absolute difference in path was 10.3 ± 4.1 mm (Table 1). The average minimum and maximum distance between paths were 4.2 ± 2.1 mm and 19.2 ± 11.1 mm, respectively. Because the cadaveric derived paths in the model were averages of multiple strands, there are some discontinuities where muscle strands terminate or originate (e.g., superior end of splenius cervicis in Figure 3).

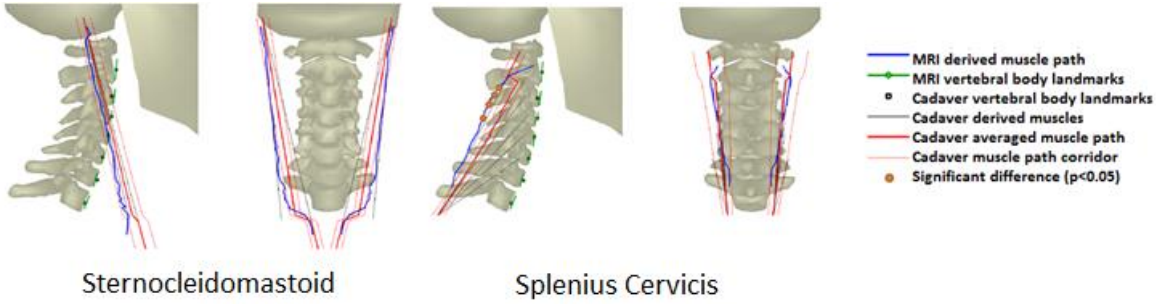

Figure 3: The cadaveric dissection derived muscle path of the sternocleidomastoid and splenius cervicis were compared against the MRI derived muscle paths. Vertebral body landmarks were used to align the results with Vasavada et al. (2008).

Table 1: Average transverse distance (mm) between model and MRI derived muscle paths for three head and neck postures in the adult model. Three muscle models were used to investigate the effect of muscle wrapping during flexion and extension bending.

Muscle	Neutral	Flexion			Extension		
		Single-Segment	Sliding Contact	Multi-Segment	Single-Segment	Sliding Contact	Multi-Segment
Levator Scapulae	7.5	12.9	5.8	5.8	4.4	5.1	5.1
Longissimus Capitis	13.1	22.8	14.5	14.5	10.5	12.0	12.1
Longissimus Cervicis	9.2	14.1	7.6	7.6	7.5	10.0	10.0
Longus Capitis	5.3	4.5	3.3	3.3	9.3	7.8	7.9
Scalenus Anterior	11.5	12.5	12.1	12.1	9.8	10.7	10.7
Scalenus Med and Post	8.7	11.7	7.3	7.3	6.7	7.7	7.7
Semispinalis Capitis	9.4	8.1	9.2	9.2	9.5	9.0	8.9
Semispinalis Cervicis	8.5	10.8	7.3	7.3	9.1	8.8	8.7
Splenius Capitis	9.1	14.8	7.7	7.7	8.9	9.7	9.7
Splenius Cervicis	12.6	18.9	8.9	8.9	10.0	13.6	13.6
Sternocleidomastoid	7.6	19.3	9.9	10.0	10.2	9.4	9.3
Trapezius	21.2	24.8	20.9	20.8	21.1	21.6	21.6
Average	10.3	14.6	9.5	9.5	9.7	10.4	10.4
Standard deviation	4.1	5.9	4.6	4.6	4.0	4.1	4.1

During flexion, muscle multi-segment and sliding contact models that simulated muscle wrapping were closer ($p < 0.05$) to the MRI derived paths than the single-segment muscle model which did not simulate muscle wrapping (Table 1). The average difference between paths was 60 ± 43% greater when no wrapping was implemented compared to when wrapping was implemented. Conversely, the models that simulated muscle wrapping were not significantly different from the single-segment muscle model during extension bending. The average difference decreased 6 ± 14% when no wrapping was implemented compared to when wrapping was implemented. The sliding contact and multi-segment muscle models, which simulate muscle wrapping, resulted in identical pathways (Table 1). Paths for the sternocleidomastoid and splenius cervicis during flexion and extension are presented in Figure 4.

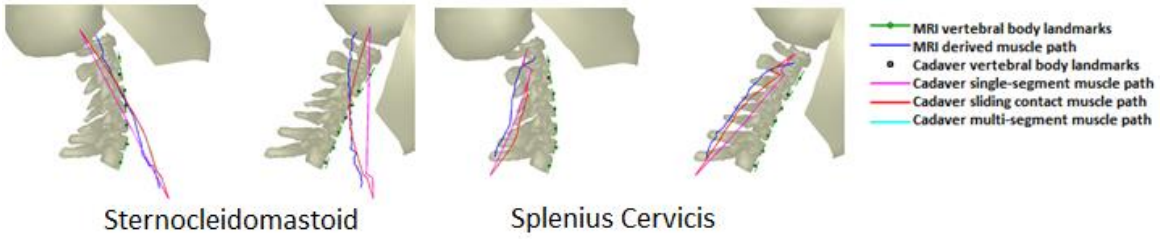

Figure 4: The cadaveric dissection derived muscle paths of the sternocleidomastoid and splenius cervicis during flexion and extension were compared against MRI derived muscle paths. The multi-segment and sliding contact model are coincident and represented by the red line.

3.2 15 G frontal impact

A comparison of the three muscle wrapping techniques to the 15 G frontal impact volunteer corridor (Figure 5) shows both multi-segment models (multi-segment and sliding contact) provide greater correlation with the volunteer response than the single-segment model, with the sliding contact model providing the highest correlation.

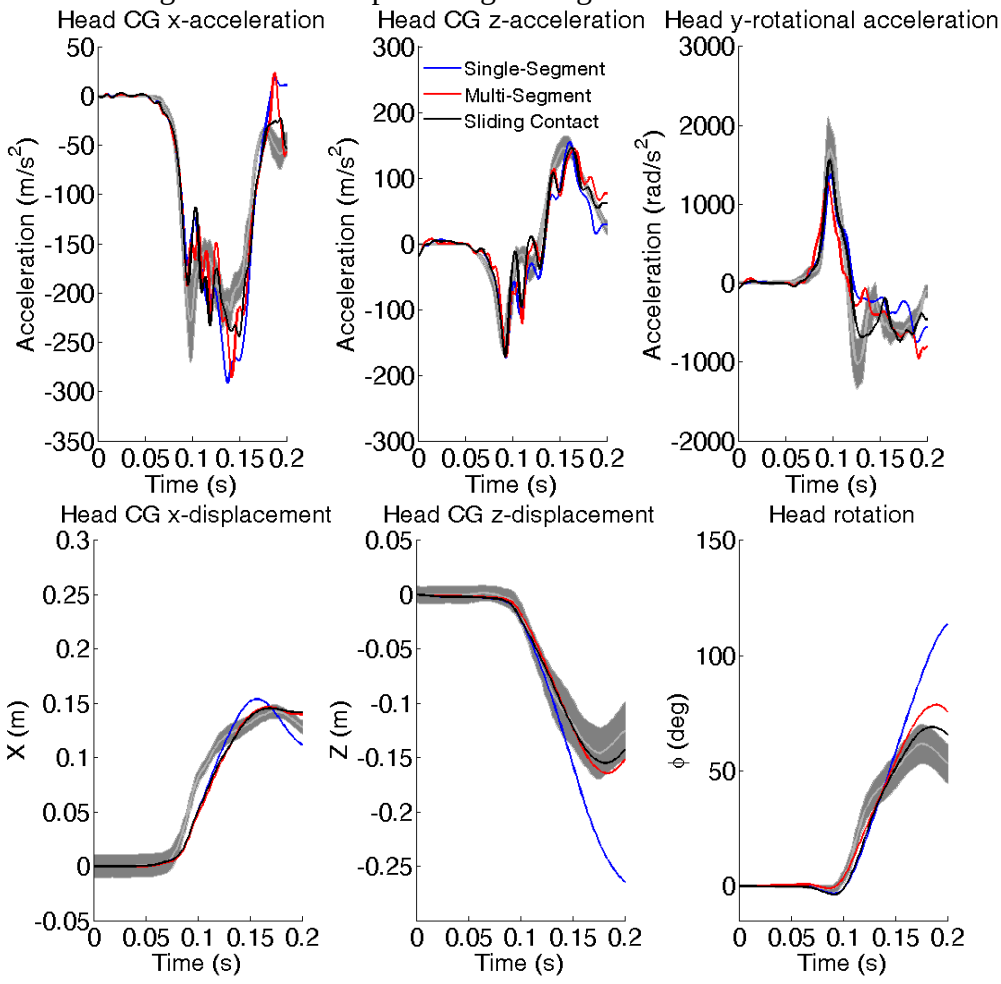

Figure 5: Adult model with full extensor activation kinematic response to 15 G frontal impact. Volunteer response is indicated by the grey corridor representing mean ± one standard deviation.

Table 2 compares peak kinematic values and correlation scores across the different muscle wrapping techniques for the full extensor case.

Table 2: Peak kinematic values for the full extensor activation for the 15 G frontal impact.

	Muscle Wrapping Technique		
	Single-Segment	Multi-Segment	Sliding Contact
Head rotation peak (deg)	114	78.6	69.0
Head rotation peak time (s)	0.200	0.189	0.185
Head rotation correlation score	0.646	0.843	**0.847**
Neck rotation peak (deg)	94.5	62.5	62.4
Neck rotation peak time (s)	0.200	0.175	0.174
Neck rotation correlation score	0.798	0.733	**0.825**
Head rotational acceleration peak (rad/s^2)	1380	1280	1570
Head rotational acceleration peak time (s)	0.098	0.095	0.097
Head rotational acceleration correlation score	0.689	0.765	**0.877**
Head lag RMS error	13.3	6.69	10.4
Head lag time (s)	0.027	0.019	0.027
Head displacement peak x (m)	0.154	0.146	0.145
Head peak x (m)	0.185	0.177	0.176
Head displacement peak x time (s)	0.157	0.168	0.169
Head displacement x correlation score	0.715	**0.820**	0.812
Head displacement peak z (m)	0.265	0.164	0.155
Head peak z (m)	-0.058	0.042	0.051
Head displacement peak z time (s)	0.200	0.183	0.182
Head displacement z correlation score	0.730	0.971	**0.985**
Head linear displacement peak (m)	0.287	0.218	0.211
Head linear displacement peak time (s)	0.200	0.180	0.179
Head linear acceleration x peak (m/s^2)	291	286	244
Head linear acceleration x peak time (s)	0.138	0.143	0.151
Head linear acceleration x correlation score	0.628	0.728	**0.754**
Head linear acceleration z peak (m/s^2)	174	171	172
Head linear acceleration z peak time (s)	0.094	0.095	0.093
Head linear acceleration z correlation score	0.727	0.708	**0.789**
Head linear acceleration peak (m/s^2)	296	304	260
Head linear acceleration peak time (s)	0.139	0.143	0.143
Head linear acceleration correlation score	0.691	0.804	**0.824**
Average global correlation score	0.712	0.823	**0.863**

Of all the muscle wrapping techniques, the sliding contact model provides the highest correlation, except in the case of peak head displacement in the x direction. The single-segment model had significantly lower correlations for all the kinematic metrics than the other

two models. The average global correlation score for each simulation (Table 3) indicates the sliding contact, full extensor case provides the highest correlation to the adult corridors. Additionally, full extensor activation always results in higher correlation with the volunteer corridors than the relaxed activation.

Table 3: Comparison of average global correlation scores.

Muscle Wrapping Technique	Activation	
	Full Extensor	Relaxed
Single-Segment	0.712	0.696
Multi-Segment	0.823	0.709
Sliding Contact	0.863	0.721

To provide a basis for comparison across the different muscle wrapping techniques and activations, peak kinematic values were tabulated. Shown in Table 4 are peak head rotation and HIC values. The single-segment muscles provided the highest rotations and HIC values, with multi-segment next, except for the relaxed activation.

Table 4: Comparison of peak head rotation (degrees) and HIC across muscle activation and muscle wrapping technique. Single-segment muscles consistently allow the largest head rotations.

	Head Rotation		HIC	
Muscle Wrapping Technique	Full Extensor	Relaxed	Full Extensor	Relaxed
Single-Segment	114	160	66.5	94.3
Multi-Segment	78.6	121	57.1	67.7
Sliding Contact	69.0	125	50.0	76.2

Peak HIC values among different activations were higher for single-segment models than those which simulated muscle wrapping. Additionally, HIC values for the relaxed activation were higher than those for the full extensor activation.

4 DISCUSSION

4.1 Muscle paths

While the paths of cervical muscles are curved as they wrap around each other and have broad origins and insertions, it was found that the overall muscle loading line of actions could be well-represented by dividing each muscle into numerous linear strands connecting the muscle's anatomically accurate multiple insertion and origin locations. The aggregate curved path from these multiple linear strands had lower error metrics than were reported by Vasavada et al. (2008) for a single linear strand.

Maintenance of anatomically correct lines of action during neck sagittal bending was accomplished by modeling muscle wrapping. Two methods of muscle wrapping were compared and produced essentially identical muscle paths. During prescribed neck flexion of 30 degrees, the lines of action for the extensor muscles resulted in significantly decreased

error metrics when either muscle wrapping technique was employed. Conversely, muscle wrapping did not have a significant effect during extension. This may be because during extension, the extensors are curved, while the flexors are relatively straight. Therefore, during extension, single-segment muscles were sufficient to capture the flexor muscle lines of action.

The primary limitation of this portion of the study was that the MRI data [9] was from a single male subject. While six of the 12 muscles studied were significantly different from the cadaveric data along the portion of their paths, it is not known if this would be true for the average of the male population.

4.2 15 G frontal impact

In the 15 G frontal impact simulation, the full extensor activations produced higher correlation than the relaxed activation. This is because the relaxed activation did not generate sufficient force to oppose the head's inertia, allowing for higher displacements than seen in the volunteers (Table 3) regardless of muscle wrapping technique. In the single-segment simulations, the head displaced and rotated much further than either the multi-segment or sliding contact models. This occurs because unlike the multi-segment models, no intermediate nodes restrict the muscle to an extensor role. During flexion rotations, some single extensors pass anterior of the joints centers of rotation and effectively become flexors. In the simulations, this resulted in increased flexion and a "locking" of the flexion rotations. As such, the single-segment models result in the lowest correlation score to the volunteers.

While the displacement-controlled simulations showed muscle wrapping is necessary to produce accurate muscle paths, it did not indicate whether the multi-segment model is sufficient. The dynamic simulations of the 15 G frontal impact illustrated that sliding contact provides a greater correlation with volunteer corridors. Additionally, high peak head center of gravity accelerations near the end of the multi-segment model simulations (Figure 5) are not seen in sliding contact simulations. This indicates that although the multi-segment models include muscle wrapping, they alter neck forces and moments since the lack of sliding allows for locking, resulting in secondary peak accelerations. This could result in mechanistic changes in injury metrics, suggesting that muscle modeling has the potential to impact injury assessment and should be examined in other modes of loading.

One limitation of this portion of the study was the use of the relaxed activation, which was optimized to minimize head center of gravity rotation and displacement under gravitational loading specifically for sliding contact muscles. However, under gravity, both the single-segment and multi-segment models resulted in lower displacements and rotations than the sliding contact muscle model. Therefore, while other optimal muscle activations exist for the single-segment and multi-segment models, the sliding contact relaxed activation was sufficient for use.

5 CONCLUSIONS

Modeling anatomically correct cervical muscle lines of action and attachments was possible by segmenting each muscle into numerous linear strands. Furthermore, correct muscle lines of action were maintained during neck flexion and extension by modeling muscle wrapping with both sliding contact and multi-segmented muscles. With anatomically correct muscle loading lines of action and attachments, the effect of muscle loads can be

investigated during modeling of injurious loading scenarios such as frontal impact. Additionally, the use of guiding nodes for sliding contact muscles instead of rigid attachments for multi-segment muscles allows for more accurate model kinematic responses compared to volunteers in a 15 G frontal impact.

Our study emphasizes that muscle attachment and paths are important to simulate correct muscular loads and lines of action in computational models of the head and neck. This study evaluated several techniques to establish muscle paths using cadaveric and MRI data, and included curved contact guided models that more accurately simulate neck muscle paths than straight line origin-to-insertion point models commonly used in automobile biomechanics. This strategy maintained anatomically correct lines of action during neck sagittal plane bending and was found to significantly improve the lines of action for extensor/flexor muscles during the application of anterioposterior loading. This curvilinear muscle response is important in tensile, compressive, and bending scenarios, and must be included to produce biofidelic model response for frontal impacts including muscle activation.

REFERENCES

[1] de Jager, M. *Mathematical head-neck models for acceleration impacts* [Ph.D. Thesis], Eindhoven University of Technology, Faculty of Mechanical Engineering; 1996.

[2] Brolin, K., Halldin, P., Leijonhufvud, I. The effect of muscle activation on neck response. *Traffic Inj Prev.* (2005) **6**(1):67-76.

[3] van der Horst, M., Thunnissen, J., Happee, R., et al. The influence of muscle activity on head-neck response during impact. *Stapp Car Crash Conference.* Vol 41st: SAE; 1997:487-507.

[4] Dibb, A.T. *Pediatric head and neck dynamic response: A computational study* [Ph.D. Thesis]. Durham, North Carolina: Department of Biomedical Engineering, Duke University; 2011.

[5] Dibb, A.T., Cutcliffe, H.C., Luck, J.F., et al. Pediatric head and neck dynamics in frontal impact: Analysis of important mechanical factors and proposed neck performance corridors for six and ten year old ATDs. *Traffic Inj Prev.* (2014) **15**(4):386-394.

[6] Dibb, A.T., Cox, C.A., Nightingale, R.W., et al. Importance of muscle activations for biofidelic pediatric neck response in computational models. *Traffic Inj Prev.* (2013) **14**(sup1):S116-S127.

[7] Chancey, V.C., Nightingale, R.W., Van Ee, C.A., et al. Improved estimation of human neck tensile tolerance: Reducing the range of reported tolerance using anthropometrically correct muscles and optimized physiologic initial conditions. *Stapp Car Crash Journal.* (2003) **47**:135-153.

[8] Knaub, K.E. and Myers, B.S. *Cervical spine muscle* 1998.

[9] Vasavada, A.N., Lasher, R.A., Meyer, T.E., et al. Defining and evaluating wrapping surfaces for MRI-derived spinal muscle paths. *J Biomech.* (2008) **41**(7):1450-1457.

[10] Suderman, B.L., Krishnamoorthy, B., Vasavada, A.N. Neck muscle paths and moment arms are significantly affected by wrapping surface parameters. *Comput Method Biomec.* (2012) **15**(7):735-744.

[11] Suderman, B.L. and Vasavada, A.N. Moving muscle points provide accurate curved muscle paths in a model of the cervical spine. *J Biomech.* (2012) **45**(2):400-404.

[12] Hedenstierna, S. and Halldin, P. How does a three-dimensional continuum muscle model affect the kinematics and muscle strains of a finite element neck model compared to a discrete muscle model in rear-end, frontal, and lateral impacts. *Spine.* (2008) **33**(8):E236.

[13] Meyer, F., Bourdet, N., Deck, C., et al. Human neck finite element model development and validation against original experimental data. *Stapp Car Crash Journal.* (2004) **48**:177-206.

[14] Jost, R. and Nurick, G. Development of a finite element model of the human neck subjected to high g-level lateral deceleration. *Int J Crashworthiness.* (2000) **5**(3):259-270.

[15] van der Horst, M. *Human head neck response in frontal, lateral and rear end impact loading: Modelling and validation* [Ph.D. Thesis]. Eindhoven, Technische Universiteit Eindhoven; 2002.

[16] Brelin-Fornari, J., Shah, P., El-Sayed, M. Physically correlated muscle activation for a human head and neck computational model. *Computer Methods in Biomechanics & Biomedical Engineering.* (2005) **8**(3):191-199.

[17] Stemper, B.D., Yoganandan, N., Pintar, F.A. Validation of a head-neck computer model for whiplash simulation. *Medical and Biological Engineering and Computing.* (2004) **42**(3):333-338.

[18] Linder, A. A new mathematical neck model for a low-velocity rear-end impact dummy: Evaluation of components influencing head kinematics. *Accident Anal Prev.* (2000) **32**(2):261-269.

[19] Kruidhof, J. and Pandy, M.G. Effect of muscle wrapping on model estimates of neck muscle strength. *Computer Methods in Biomechanics & Biomedical Engineering.* (2006) **9**(6):343-352.

[20] Vasavada, A.N., Li, S., Delp, S.L. Influence of muscle morphometry and moment arms on the moment-generating capacity of human neck muscles. *Spine.* (1998) **23**(4):412-422.

[21] van Lopik, D.W. and Acar, M. Development of a multi-body computational model of human head and neck. *Proceedings of the Institution of Mechanical Engineers. Part K, Journal of multi-body dynamics.* (2007) **221**(2):175.

[22] Williams, J.L. and Belytschko, T.B. A three-dimensional model of the human cervical spine for impact simulation. *Journal of Biomechanical Engineering.* (1983) **105**(4):321-331.

[23] Ewing, C.L. and Thomas, D.J. *Human head and neck response to impact acceleration*: DTIC Document; 1972.

[24] Xu, L., Agaram, V., Rouhana, S., et al. *Repeatability evaluation of the pre-prototype nhtsa advanced dummy compared to the Hybrid III*, (2000).

[25] Panzer, M.B., Fice, J.B., Cronin, D.S. Cervical spine response in frontal crash. *Med Eng Phys.* (2011) **33**(9):1147-1159.

[26] Gehre, C., Gades, H., Wernicke, P. Objective rating of signals using test and simulation responses. Paper presented at: 21st International Technical Conference on the Enhanced Safety of Vehicles Conference (ESV)2009.

[27] Pedotti, A., Krishnan, V., Stark, L. Optimization of muscle-force sequencing in human locomotion. *Math Biosci.* (1978) **38**(1-2):57-76.